CHAPTER 113

REDUCTION PROCESS OF CROSS-SECTIONAL AREA AT RIVER MOUTH

Takuzo Shimizu*, Kosuke Kondo** and Ryoichi Kajima***

ABSTRACT

Reduction processes of the cross-sectional area at a river mouth were investigated on the basis of numerical simulations and field measurements, in order to predict the possibility of closing of the mouth of the Samegawa River, Fukushima, Japan. As a result, it was found that the decrease in tidal prism, induced by a reduction of the cross-sectional area, had an important effect on the closing of the river mouth. By considering this effect and estimating the sediment transport rate properly, a practical prediction model was successfully established for simulating the reduction processes of the crosssectional area at the river mouth.

1. INTRODUCTION

A jetty was constructed on the northeastern side at the mouth of the Samegawa River, Fukushima, Japan, in order to prevent increased heated water from the Nakoso Thermal Power Station from affecting the river's fishery. After the jetty construction, the heated water is separately and directly discharged into the Pacific Ocean through an open channel excavated about 500 m northeast of the river mouth through the sand spit which extends along the shore in front of the power station (Figure 1).

One of the most important influences of the jetty construction is the reduction of the cross-sectional area at the river mouth, induced by the decreased discharge passing through it. However, since many factors, such as waves, nearshore currents, tidal flows, inherent river flows, and heated water discharge are involved in complicated sediment transport around the river mouth, beach changes or closing processes near the river mouth are not yet completely predictable.

This study aims to elucidate the mechanism of the interaction between hydraulic factors, especially tidal change and topographical changes at the river mouth, and to establish a prediction model of the reduction processes of the cross-sectional area.

*** Chief Engineer, Central Research Institute of Electric Power Industry, 1646 Abiko, Abiko City, Chiba 270-11, Japan.

^{*} Engineer, Design and Engineering Department, Penta-Ocean Construction Co., Ltd., 2-2-8 Koraku, Bunkyo-ku, Tokyo 112, Japan.

^{**} Principal Engineer, Design and Engineering Department, Penta-Ocean Construction Co., Ltd., 2-2-8 Koraku, Bunkyo-ku, Tokyo 112, Japan.

2. OUTLINE OF FIELD INVESTIGATION

2.1 Study Area

Field investigations were carried out around the mouth of the Samegawa River, located on the Pacific coast in the southern part of Fukushima Prefecture (Figure 1). The sandy beach stretches from southwest to northeast in front of the river mouth. A rocky shoal exists only near the Ryugu Headland at the northeast end of the shore. The bottom contours are parallel to the shoreline and the bottom slope is as gentle as 1/70. The Samegawa River is a small and rapid river having a catchment area of 600.9 km² and an average bottom slope of 1/50 to 1/70. The river surface area influenced by tides was about 73,400 m² before the jetty construction and now is about 53,600 m².

According to the wave climate data observed by the Ministry of Transport over a five-year period from 1981 to 1985 off the Onahama Harbour, about 9 km northeast of the study area, the mean significant wave height is 1.0 m, the mean significant wave period is 8.1 s, and the occurrence frequency of wave heights beyond 2.0 m is less than 6 %. Wave directions, obtained by visual observations twice daily with a transit from the roof of the Power Station, are limited from ESE to SSE. The dominant direction is SE, normal to the shore, and its frequency reaches about 81 %.

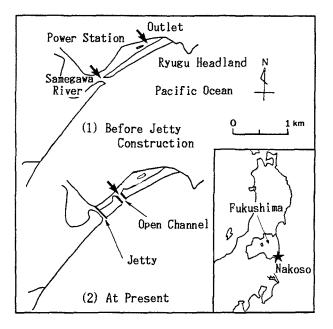


Figure 1 Study Area Location Map.

2.2 Field Investigation Program

The jetty construction was undertaken in August 1982 and completed in May 1985. Field investigations were carried out over a period of approximately five years, beginning in October 1980. The field investigation program consisted of:

- (1) coastal topography surveys (about 4 times/year),
- (2) cross-sectional area surveys at the river mouth (about once a month),
- (3) 25-hour continuous readings of current and water level, during which water temperature and salinity were measured twice (16 times/5 yeras),
- (4) nearshore current observations (occasional), and
- (5) fluorescent sand tracer experiments (3 times/5 years).

Topographical changes and hydraulic characteristics were studied mainly using the data obtained in (2) and (3) above.

3. TOPOGRAPHICAL CHANGES AT RIVER MOUTH

3.1 Position of River Mouth

Figure 2 shows aerial photographs of the past and the present around the mouth of the Samegawa River. The position of the mouth before the jetty construction had a tendency to shift toward the northeast. Before the extreme flood event in September 1977, it had been located at the Ryugu Headland about 1.5 km northeast from the present position. This shift of the river mouth location is because the most effective wave energy arrives from the southeast direction, driving the net littoral sediment transport northeastward.

In the fluorescent sand tracer experiments carried out twice on the southeastern shore, most of the tagged grains were found along the shoreline extending from the injection points to the river mouth, although longshore currents were not always directed to the northeast. This is attributed to many complicated influences of the incident wave direction, the tidal elevation, the sea-bed topography, the river discharge and so on. This result suggests that not only the longshore currents but also the sediment transport in the swash zone play important roles in the sand spit extension around the river mouth.

3.2 Change of Cross-sectional Area

Figure 3 shows time histories of the cross-sectional area A from October 1980 to March 1985, together with variations of wave energy flux P, inherent river discharge Qr, and heated water discharge Qp. The solid curves in the corss-sectional area diagram are the results of simulations mentioned later.

It is seen in this figure that the cross-sectional area was forcibly and abruptly enlarged by every extreme flood event. After that it was gradually reduced and finally came to a state of dynamic equilibrium. This kind of variation pattern is common and repeated.

COASTAL ENGINEERING-1986



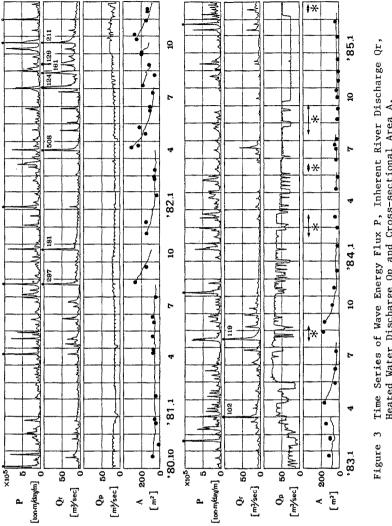
(1) 1980.9.30



(2) 1986.5.27

Figure 2 Aerial Photographs of Study Area.







The equilibrium area was about 50 m^2 before the jetty construction but after then decreased to about 20 m^2 because of the decrease in the total discharge passing through the river mouth caused by the separation of the heated water. Recently, maintenance dredgings have been carried out a few times a year, but not during fishing seasons for sweetfish in spring and salmon in autumn. The cross-sectional area was at the minimum of 11.8 m^2 with a width of 12.7 m in November 1984. This is partly because it was during the salmon fishing season and, importantly, because there were no extreme flood events throughout the year.

Next we investigate shape characteristics of the cross-section. The relationship between the area and the width of the minimum cross-section is close to that of a triangular cross-section rather than that of rectangular one (as Ogawa et al. (1984) has already pointed out). We however assume that the cross-section is rectangular, in order to make easy the use of the relationship between the width and the mean depth in numerical simulations.

The relationships between the cross-sectional area A and the width B or the mean depth h were calculated on the basis of the field surveys by regression analysis. The results are shown as follows:

 $B = 1.83 \text{ A}^{0.8} \quad (\text{correlation coefficient 0.91}) \quad (1)$

 $h = 0.55 A^{0.2}$ (correlation coefficient 0.48) (2)

The width shows a fairly good correlation with the area. On the other hand, the mean depth data observed after the jetty construction scatter around the above relationship. This is because the increased river discharge causes scouring adjacent to the jetty instead of enlarging the width.

4. HYDRAULICS AT RIVER MOUTH

4.1 Water Level and Discharge at River Mouth

The water level and the discharge at the river mouth are affected mainly by tidal flows and inherent river flows, aside from the wave set-up. Especially the tidal flow was supposed to be predominant under ordinary conditions but not during extreme flood events. To examine this, sixteen field observations were carried out, in which both the water level and the horizontal velocities were measured for 25 hours running, mainly during spring tide. In this section we report results of the above measurements.

Two or three two-component electro-magnetic current meters were placed about 1 m above the bottom on the minimum cross-section of the river mouth. In order to determine the ratio of the mean velocity at the measurement points to the cross-sectionally averaged velocity, another way of measurement using a propeller-type flowmeter was carried out at about 20 to 30 points spaced on the same cross-section once during flood tide and once during ebb tide. In every case there was no evidence of much spatial asymmetry in the flow, and therefore it can be

1540

considered that data obtained by the electro-magnetic current meters were representative of the cross-sectionally averaged velocities. The water level variations were measured every 30 or 60 minutes by visual observation using poles installed near the electro-magnetic current meter.

Figure 4 shows an example of time series of the water level and the discharge at the river mouth. The highest water level is approximately equal to the coean's high tide level, whereas the lowest does not fall to the ocean's low tide level. Although the ocean tide changes nearly sinusoidally, the water level at the river mouth changes asymmetrically with the ebb period being longer than the flood period.

Figure 5 shows the relationship between the measured high and low water levels at the river mouth and those calculated by the Meteorological Agency at Onahama Harbour. Figure 5 indicates that the above-mentioned tendency becomes apparent when the width of the river mouth is less than approximately 60 m.

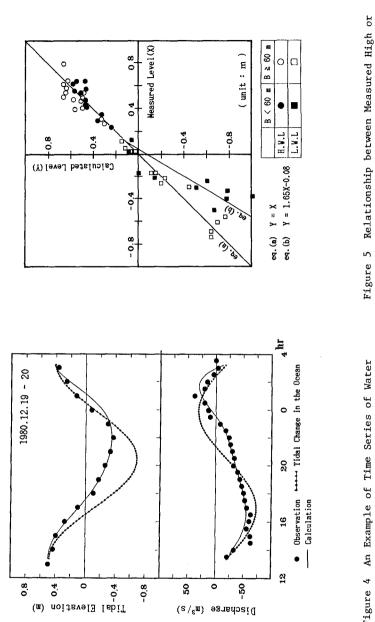
Tidal prism is defined, in general, as the gross volume of water entering or exiting an inlet during ebh or flood tides. According to the results of the field observations, it has been confirmed that tidal prism can be estimated by multiplying the difference of water level change at the river mouth by the river surface area under the influence of tides. Therefore, the decrease in tidal range results in a substantial decrease in tidal prism.

Table 1 lists mean annual values of inherent river discharge, heated water discharge, tidal discharge, and total discharge passing through the river mouth. The total discharge was calculated at the sum of the former three. Since the jetty construction in 1983, there has been no heated water discharge through the river. The tidal discharge was estimated by the following method:

- (1) The lowest water level at the mouth is estimated by using the two different relations, equation (a) and (b), according to the width beyond or below 60 m as shown in Figure 5.
- (2) The tidal prism during a half tidal cycle is calculated by multiplying the difference between the highest and the lowest water levels by the river surface area.
- (3) The tidal discharge is then obtained by averaging the tidal prism over the half tidal cycle.

The tidal discharge thus calculated is not strictly true becuase the ebb and flood periods are assumed to be equal, ignoring the actual difference between the two.

The total flow rate passing through the river mouth decreased from a yearly average value of 50 to 60 m³/s before the jetty construction to about 20 m³/s after the construction. This is not only because the heated water was separated, but also because the decrease in the river surface area induced the decrease in tidal prism.





Low Water Levels and Those Calculated.

	1980.10 -1981.3	1981.4 -1982.3	1982.4 -1983.3	1983.4 -1984.3	1984.4 -1985.3		
Inherent River Discharge	7.6	9.6	15.1	7.2	3.9		
Heated Water Discharge	16.0	15.7	21.2	(60.6)*	(37.6)*		
Tidal Discharge	25.9	23.3	22.3	16.3	15.4		
Total Discharge	49.5	48.6	58.6	23.5	19.3		
				(uni	(unit: m3/s)		

Table 1 Mean Annual Values of Inherent River Discharge, Heated Water Discharge, Tidal Discharge and Total Discharge Passing through the River Mouth.

* heated water discharge through the new open channel

4.2 Numerical Model

As discussed in the preceeding section 4.1, the water level at the river mouth does not fall as low as the sea water level during ebb tide. As a result the tidal prism decreases so that the width of the river mouth is reduced to less than about 60 m. In the Samegawa River the inherent river discharge is small and the tidal prism shares 70 to 80 % of the total flow rate.

In this section we estimate the decrease in tidal prism by taking into account head losses due to friction and at the entry, exit and bend.

The numerical model developed in this study is essentially similar to that used in the analysis of a sea-inlet-bay system (e.g. see Bruun (1978)). Consider such a model of the river mouth as the tidalinfluenced water surface area connected with the sea through a channel with uniform rectangular cross-section. Assuming that the velocity in the channel is constant and that the tidal wavelength is much larger than the channel length, the one-dimensional equation of motion along the channel axis can be expressed as:

$$du/dt + gdn/dx + I_{f} + I_{o} = 0$$
(3)

 $d\eta/dx = (\eta - \eta s)/2\ell$ (4)

$$I_{f} + I_{g} \approx g n^{2} |u|u / R^{4/3} + fc |u|u / 2l$$
 (5)

where u is the average velocity (positive into the upstream direction), g is the acceleration of gravity, n is the water level at the river mouth, ns is the sea water level, ℓ is the channel length, A is the cross-sectional area, I_f is the bottom friction term, I_{ℓ} is the term of head losses except frictional loss, R is the hydraulic radius, n is Manning's friction coefficient, and fc is the head loss coefficient at the entry, exit and bend. The continuity equation can be used as expressed in equation (6), assuming that the river water level rises and falls uniformly at any time.

$$A u + Qr = S d\eta/dt$$
(6)

where A is the cross-sectional area, Qr the inherent river discharge, and S the river water surface area taken as independent of the water level. The validity of equation (6) has been verified in the practical sense by field measurements.

Relating equations (4), (5) and (6) to (3) and eliminating the velocity u, the following ordinary differential equation of the second order with respect to η can be obtained.

$$\frac{d^2\eta}{dt^2} + \left\{ \left(\frac{fc}{2\ell} - \frac{g}{R^4/3} \right) \frac{s}{A} \left| \frac{d\eta}{dt} - \frac{Qr}{s} \right| - \frac{B}{A} \frac{d\eta}{dt} \right\} \left(\frac{d\eta}{dt} - \frac{Qr}{s} \right) + \frac{Ag}{S\ell} (\eta - \eta s) = 0 \quad (7)$$

in which the time variation of Qr is assumed to be slow enough to ignore. Equation (7) can easily be solved numerically by using the Runge-Kutta-Gill method. The stationary solution can be obtained by calculating repeatedly for several tidal cycles from certain initial conditions. The initial conditions used in this model are $\eta = \eta s + \Delta \eta$, $d\eta/dt = Qr/A$, at t = 0, where $\Delta \eta$ is the displacement of backwater given by the result of non-uniform flow calculation. The sea tide is assumed to be sinusoidal.

Calculation of the variation of the water surface elevation by the above method leads to the result that the high water in the river becomes lower than that in the ocean and the time of high water in the river lags behind that in the ocean. These are natural results caused by nonlinear head losses and are observed in a general sea-inlet-bay system. However, these results are inconsistent with those of the field measurements, which indicate that both the high water level and its time in the river are approximately equal to those in the ocean. Probably, this is because the depth of the channel and the depth of the river surface area influenced by the tide are not large enough as compared with the ocean tidal range. Therefore, the variation of the water level at the river mouth from the time of the ocean's high tide elevation is calculated under the initial conditions, as mentioned previously, whereas it is approximated using an appropriate fifth-order function, from the time when the calculated level becomes lowest or equal to the ocean's tide, to the time of the next high water level.

An example of the result of the numerical simulation is shown in Figure 4. The solid curves show the calculated time series of water level and discharge at the river mouth. In spite of simplicity of the model presented here, the calculated values correlate well with the observed ones. In the other cases, the decrease in tidal prism can be estimated within ± 10 % error by properly choosing the head loss coefficient fc and the channel length ℓ .

4.3 Effect of Decrease in Tidal Prism

This section presents effects of the width variation on the total discharge and the sediment transport rate at the river mouth by using the numerical model discussed in section 4.2.

First the variation of the absolute flow volume during a tidal cycle (12.5 hours) as caused by the change in the width is investigated. The relationship between the width and the mean depth obtained in section 3.2 is used.

Figure 6 shows the results of three cases of tidal ranges:(1) 1.45 m of the mean spring tidal range, (2) 0.91 m of the range between the mean higher high and the lower low water levels, and (3) 0.33 m of the mean neap tidal range, with no inherent river discharge. The discharge passing through the river mouth decreases exponentially as the width decreases. For example, at spring tide when the width is 5 m, the discharge decreases to about one third that for conditions of 100 m width, in which the water level at the river mouth changes simultaneously with that in the ocean.

Next, the effect of the width variation on the gross volume of sediment transport rate for a tidal cycle is shown in Figure 7, in which comparison is made with that in the cases of the same tidal change at the river mouth as that in the ocean. A Bagnold-type formula, equation (8), proposed by Watanabe (1982) was used to calculate the transport rate.

$$q_{r} = K_{r} \left(u_{\star}^{2} - u_{\star c}^{2} \right) |u| /g$$
 (8)

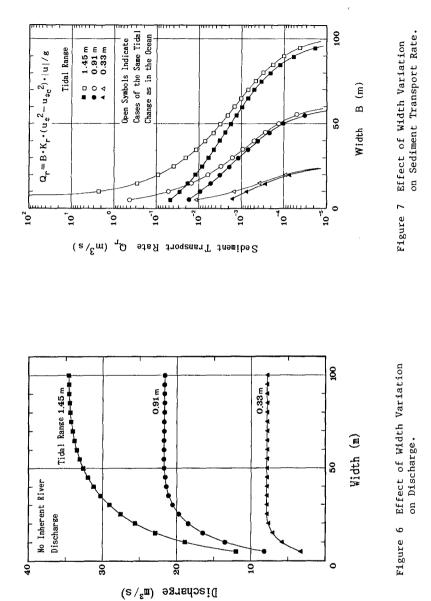
in which q_r is the volume transport rate including the sediment porosity, u_{\star} is the friction velocity, u is the flow velocity, and K_r is the dimensionless coefficient. The assumptions used in this calculation are (1) the critical Shields parameter is 0.06, (2) the grain diameter is 0.25 mm, (3) the dimensionless coefficient K_r is 1.0, and (4) the friction velocity is estimated using the turbulent logarithmic velocity profile law.

It is generally seen that the sediment transport rate increases rapidly as the width decreases, because the flow becomes fast. However, when the width becomes narrower to some extent, the sediment transport rate is forced to become much smaller than that in the case of the same tidal change as in the ocean. For example, it becomes 1/10to 1/100 at spring tide when the width is less than 20 m.

5. NUMERICAL SIMULATION OF REDUCTION PROCESS OF CROSS-SECTION

5.1 Prediction Model

Shuto and Aota (1980) originally proposed a numerical model predicting the time variation of the cross-sectional area at a river mouth and Ogawa et al. (1984) further developed the model. In these models the cross-sectional area was assumed to change owing to sediment



outflow caused by the river flow and sediment inflow caused by waves (as shown in Figure 8). However, vagueness remains in the physical meaning of the two coefficients involved in the sediment transport formulas; i.e. values of the coefficients suitable for the observed changes are different for different periods at the same place.

We now introduce the effect of the decrease in tidal prism, induced by a reduction of the cross-sectional area at the river mouth, into the prediction model. In this model the instantaneous sediment outflow caused by the river flow is calculated using the water level and velocity estimated by the numerical hydraulic model (discussed in section 4.2) and the total volume of sediment outflow over a tidal cycle from the high tide to the next high tide is evaluated. On the other hand, the volume of sediment inflow is estimated using the wave conditions at the breaking point. Then the variation of the crosssectional area is simulated for every tidal cycle on the basis of the balance of the two kinds of sediment transport.

The governing equation for sediment mass conservation at the river mouth is expressed as

$$L dA/dt = q B - q B$$
 (9)

in which q_r , q_w are the volume transport rates of sediment outflow and inflow, L is the width of the sand spit, A is the cross-sectional area, and B is the width of the river mouth.

The sediment outflow is given by equation (8), and assumed to act so as to maintain the cross-section independently of the flow direction.

The sediment inflow is simply expressed by equation (10), because it is difficult to estimate it quantitatively by taking account of the mechanism of sand motion.

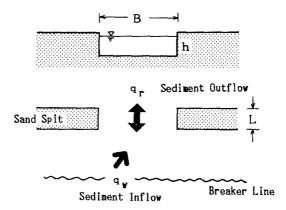


Figure 8 Schematic Diagram of Sediment Transport at River Mouth.

$$\mathbf{q}_{\mathbf{w}} = \mathbf{K}_{\mathbf{w}} \mathbf{H}_{\mathbf{b}}^{1.5} \tag{10}$$

in which H_b is the significant wave height at the breaking points, and K_w is a dimensional coefficient. This expression is obtained by considering that the sediment transport rate in the surf zone is proportional to the wave energy flux at the breaker line and dividing it by the width of the surf zone. The breaker height H_b is estimated using the following formula proposed by Sunamura (1983), b

$$H_{\rm b}/H_{\rm o} = (\tan\beta)^{0.2} (H_{\rm o}/L_{\rm o})^{-0.25}$$
 (11)

where H_O is the significant wave height in deepwater, L_O is the wavelength in deepwater, and tan β is the bottom slope.

According to the results of the previous studies and the fluorescent sand tracer experiments, the coefficients $K_{\rm r}$ and $K_{\rm w}$ are expected to be of the order of magnitude of 10^0 and 10^{-5} respectively.

The reults of the simulation are shown in Figure 3. Calculation was terminated during extreme flood events causing the abrupt enlargement of the cross-section, and during dredging. With constant values of the coefficients, $K_r = 1.0$ and $K_w = 2.5 \times 10^{-5}$ (m^{0.5}/s), the results show a good agreement with the observed changes in the reduction processes at the river mouth. These values of the coefficients used in the simulation are the same order of magnitude with those mentioned above.

5.2 Possibility of River Mouth Closing

In order to examine the possibility of closing, the relationship between the significant wave height in deepwater and the width of the river mouth in a state of dynamic equilibrim (dA/dt = 0) is investigated. Figure 9 shows the results obtained under three conditions of tidal ranges with no inherent river discharge. When the wave height is placed above the curve of a reference tidal range at a reference width, the cross-sectional area becomes smaller and in the opposite case it becomes larger.

Since the width of the Samegawa River is now 10 to 30 m, it can be seen that the mouth of the river expands and contracts repeatedly in response to waves and tides. Therefore, it can be concluded that the present cross-section reaches an approximate equilibrium and that complete closure will not occur.

6. CONCLUDING REMARKS

As a result of this study based on the field measurements as well as numerical simulations, it has been found that the closing process has the following mechanism: a cycle that commences with a reduction of the cross-sectional area induces a decrease in tidal prism resulting in a substantial decrease in sediment outflow, and this decreased sediment outflow causes a further reduction of the cross-sectional area as the last phase before another cycle begins again. By considering this

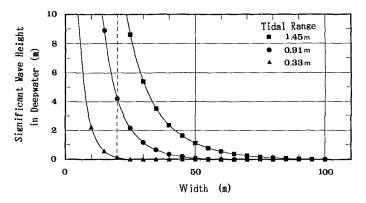


Figure 9 Relationship between Significant Wave Height in Deepwater and Width of River Mouth in a State of Dynamic Equilibrium.

mechanism, it has become possible to reasonably simulate the topographical changes of the river mouth.

However, the prediction model of the reduction process presented here is a simple one-dimensional model and it is impossible to simulate the variation of the sand spit width. Therefore, it is important to properly choose such parameters as to represent the plane configuration of the sand spit and the cross-sectional shape of the channel, on the basis of topographical surveys.

ACKNOWLEDGEMENTS

We would like to express our deep appreciation to H. Kaburagi and Y. Matsubara of the Joban Joint Power Co., Ltd. for the support they lent to this study and for their permission to publish this paper. We would also thank Prof. A. Watanabe of University of Tokyo for his useful suggestion in preparing the manuscript.

REFERENCES

- Bruun, P. (1978) : Stability of Tidal Inlets, Theory and Engineering, Elsevier Scientific Publishing Company, pp.83-108.
- Ogawa, Y., Y. Fujita and N. Shuto (1984) : Change in the Crosssectional Area and Topography at River Mouth, Coastal Engineering in Japan, Vol.27, pp.233-247.
- Shuto, N. and S. Aota (1980) : Numerical Simulation of the Seasonal Variation in the Cross-sectional Area at River Mouth, Coastal Engineering in Japan, Vol.23, pp.205-217.
- Sunamura, T. (1983) : Determination of Breaker Height and Depth in the Field, Annual Report, Institute of Geoscience, University of Tsukuba, No.8, pp.53-54.
- Watanabe, A. (1982) : Numerical Models of Nearshore Currents and Beach Deformation, Coastal Engineering in Japan, Vol.25, pp.147-161.